Short Communication

Improvement of the Magnetic Properties and Corrosion Resistance of Ga-doped MnBi Alloys

Changquan Zhou[1], and Minxiang Pan[2,]*

[1] Zhejiang University of Water Resources and Electric Power, Hangzhou 310018, China
[2] Magnetism key laboratory of Zhejiang Province, China Jiliang University, Hangzhou 310018, China
[*]E-mail: panminxiang@cjlu.edu.cn

$MnBi_{1-x}Ga_x$ (x = 0 ~ 0.5) alloys have been fabricated by melt spinning with substantial heat treatment. The effect of Ga content on the microstructure and magnetic properties of these alloys are systemically investigated. The optimal magnetic properties ((BH)$_{max}$: 0.67 MGOe) are obtained for the Ga-doped (x = 0.1) in terms of the combined effect of coercivity H_{cj} and remanence M_r. Compared to the Ga-free alloy, the remanence and maximum energy product of the Ga-doped (x = 0.1) increase slightly. When x > 0.1, the M_r and (BH)$_{max}$ of the alloys decrease gradually, which is mainly due to the content of LTP-MnBi is decreasing with the increase of Ga content. Besides, a remarkably improvement in electrochemical stability and corrosion resistance for the Ga-doped MnBi alloys by due to the smaller grain size and uniform distribution of magnetic phases. However, the Curie temperature and the phase transition temperature of MnBi alloy decreases with the increase of Ga content.

Keywords: MnBi; Corrosion; Magnetic properties; Microstructure

1. INTRODUCTION

In recent years, with the decrease of rare earth resources and the rapid increase of prices in the world, the timely development of a new type of high magnetic rare earth-free permanent magnet is the requirement of the development of magnetic products [1-3]. MnBi permanent magnet has the advantages of low price, non-corrosive and good mechanical properties. Especially, MnBi permanent magnet has a positive coercivity coefficient in a certain temperature range, which can make up for the shortcomings of NdFeB permanent magnet [4,5]. In order to obtain magnetic materials with low coercivity temperature coefficient or even zero coercivity temperature coefficient and high permanent magnetic properties, the MnBi alloy can be mixed with NdFeB alloy to make composite magnet. That is of great significance to the development of high-temperature working motors [6,7]. There are many phase structures in MnBi alloys, among which high temperature phase (HTP) has excellent magneto-

optical properties, while low temperature phase (LTP) has high magneto-crystalline anisotropy ($K \approx 10^6$ J/m^3) [8-10]. The low temperature phase of MnBi has NiAs crystal structure and strong ferromagnetism at room temperature. It has a positive coercivity temperature coefficient in the temperature range of 150 K to 550 K [11]. The magnetocrystalline anisotropy energy of MnBi is 16 Mergs/m^3 at the room temperature and increases with the increase of temperature. At 490 K, the magnetocrystalline anisotropy energy constant reaches 22 Mergs/m^3 [12], which is higher than Nd$_2$Fe$_{14}$B magnetocrystalline anisotropy energy constant at the same temperature, it is considered to be a very potential permanent magnet material. The MnBi alloy has high coercivity at high temperature (for example, the intrinsic coercivity of the prepared binary MnBi permanent magnet alloy is 1345 kA/m at room temperature and 2547 kA/m at 300 C), it can be used in high temperature and strong demagnetization environment. Therefore, MnBi alloy is considered as a high temperature permanent magnet material with wide application prospects. Meanwhile, it is difficult to prepare pure low temperature phase under the current technical conditions. Up to now, the purity of low-temperature phase in MnBi alloy is less than 95%, which leads to the low magnetic properties of the alloy. Furthermore, as the reason of the low-temperature phase of MnBi is formed by peritectic reaction, it is extremely difficult to prepare single-phase alloys, which results in low magnetic properties and limits the application of such materials.

In order to further improve the magnetic properties of the MnBi alloys, the MnBi$_{1-x}$Ga$_x$ (x = 0, 0.1, 0.2, 0.3, 0.4 and 0.5) alloys with different Ga-doped fabricated by the by melt spinning were systemically studied in this paper. In addition, the effect of Ga content on the microstructure, magnetic properties and corrosion resistance of MnBi$_{1-x}$Ga$_x$ alloys are also discussed in detail. It is helpful for investigate the effect of Ga on the phase formation structure in MnBi magnet with the proper substitution of Ga for Bi.

2. EXPERIMENTAL PART

MnBi$_{1-x}$Ga$_x$ (x = 0, 0.1, 0.2, 0.3, 0.4 and 0.5) alloys were prepared by arc-melting with high purity of Mn (99.9%), Bi (99.99%) and Ga (99.98%) in the argon atmosphere. The melt-spun ribbons alloys were produced by melt spinning (wheel speed of 35 m/s) and then annealed at 550 K for 30 min to develop the low-temperature MnBi phase.

The phase constitution of the annealed MnBi$_{1-x}$Ga$_x$ (x = 0, 0.1, 0.2, 0.3, 0.4 and 0.5) ribbons was characterized by X-ray diffraction (XRD). The magnetic properties of the alloys were measured by using a vibrating-sample magnetometer (VSM) with a maximum applied field of 2.0 T. The microstructure of the annealed MnBi$_{1-x}$Ga$_x$ (x = 0 and 0.1) ribbons was performed by Transmission electron microscope (TEM). The polarization curves of the the annealed MnBi$_{1-x}$Ga$_x$ (x = 0 and 0.1) ribbons were measured with PARSTAT 2273 advanced electrochemical system with a scan rate of 2 mV/s and in 2.5 wt.% NaCl aqueous solution.
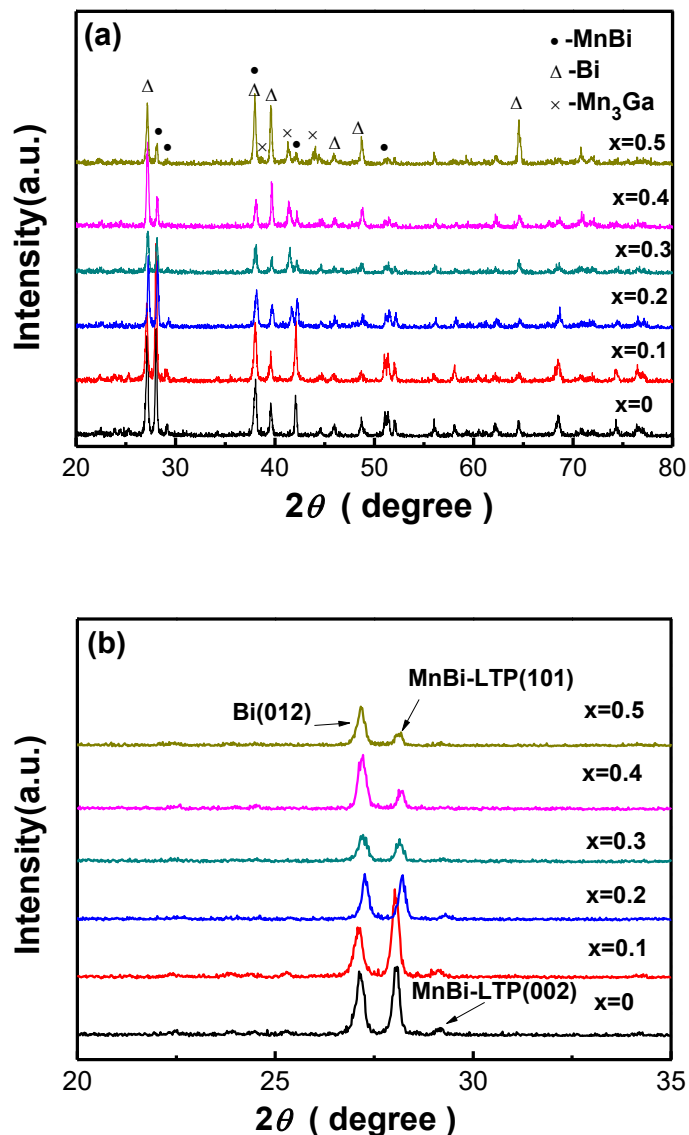
3. RESULTS AND DISCUSSION

Figure 1. (a) XRD patterns of the MnBi$_{1-x}$Ga$_x$ (x = 0, 0.1, 0.2, 0.3, 0.4 and 0.5) alloys, (b) the enlargement of the XRD pattern at 2θ = 20-35 °.

The XRD patterns of the MnBi$_{1-x}$Ga$_x$ (x = 0, 0.1, 0.2, 0.3, 0.4 and 0.5) alloys are shown in Fig. 1. It shows that the LTP-MnBi phase and Bi phase are observed for the MnBi$_{1-x}$Ga$_x$ alloys with x = 0 and x = 0.1, indicating that a small amount of Ga-doping cannot bring about new phase. With the further increase of Ga content, the intensity peaks of Mn$_3$Ga phase begins to emerge and the relative intensity gradually increases.
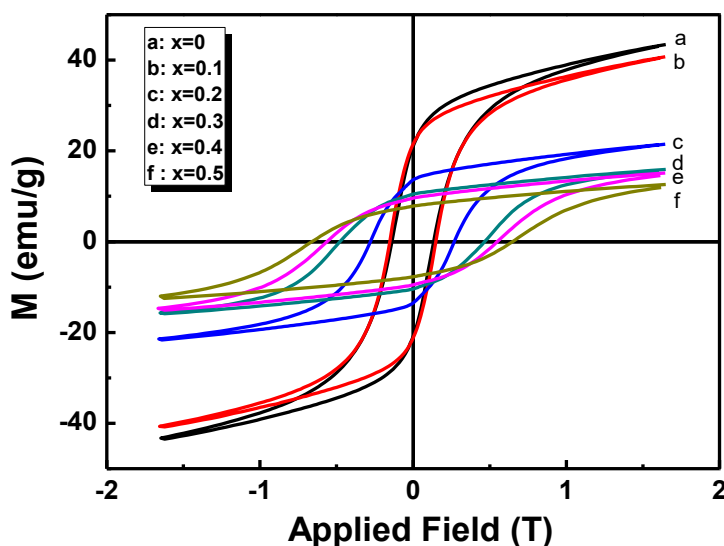
Figure 2. Hysteresis loops f $MnBi_{1-x}Ga_x$ (x = 0, 0.1, 0.2, 0.3, 0.4 and 0.5) alloys with different Ga contents.

Meanwhile, according to the enlargement of the XRD pattern at $2\theta = 20\text{-}35\,°$ in Fig. 1 (b), it shows that the with the increase of Ga doping, the relative intensity of diffraction peaks for the LTP-MnBi phase decreases gradually and shifts to the right. Based on the broadening of diffracting peaks by employing the Williamson-Hall method [13], the average grain size of the LTP-MnBi phase is 45 nm for the Ga-free (x = 0) and 15 nm for the Ga-doped (x = 0.1) alloys, it suggests that the grain size of the $MnBi_{1-x}Ga_x$ alloys can be refined with proper Ga content.

Fig. 2 presents hysteresis loops of $MnBi_{1-x}Ga_x$ alloys with different Ga contents. It shows that the hysteresis loops of the $MnBi_{1-x}Ga_x$ samples present no kink and have a uniform reverser with a single hard-magnetic phase behavior, suggesting that the good exchange-coupling between magnetic phases in these $MnBi_{1-x}Ga_x$ alloys [14,15]. Meanwhile, the saturation magnetization M_s decreases and the intrinsic coercivity H_{cj} increases with the increase of Ga content. The relationship between coercivity H_{cj}, remanence M_r and maximum magnetic energy product $(BH)_{max}$ of the samples and Ga content is shown in Fig. 3. With the increase of x, the coercivity increases gradually and reaches the maximum value (H_{cj}: 0.664 T) with x = 0.5, which is 4.8 times that of the Ga-free alloy (H_{cj}: 0.138 T). The increase of the coercivity may due to that the addition of Ga for Bi can improve the anisotropy field of the MnBi alloy, similar behavior were also reported by Zhang et al. [16] for the Mn-Bi-Ti alloys. Compared to the Ga-free alloy, the remanence and maximum energy product of the Ga-doped (x = 0.1) increase slightly. When x > 0.1, the M_r and $(BH)_{max}$ of the alloys decrease gradually, which is mainly due to the content of LTP-MnBi is decreasing with the increase of Ga content. That is consistent with previous XRD results. The optimal magnetic properties $((BH)_{max}$: 0.67 MGOe) are obtained for the Ga-doped (x = 0.1) in terms of the combined effect of coercivity H_{cj} and remanence M_r.
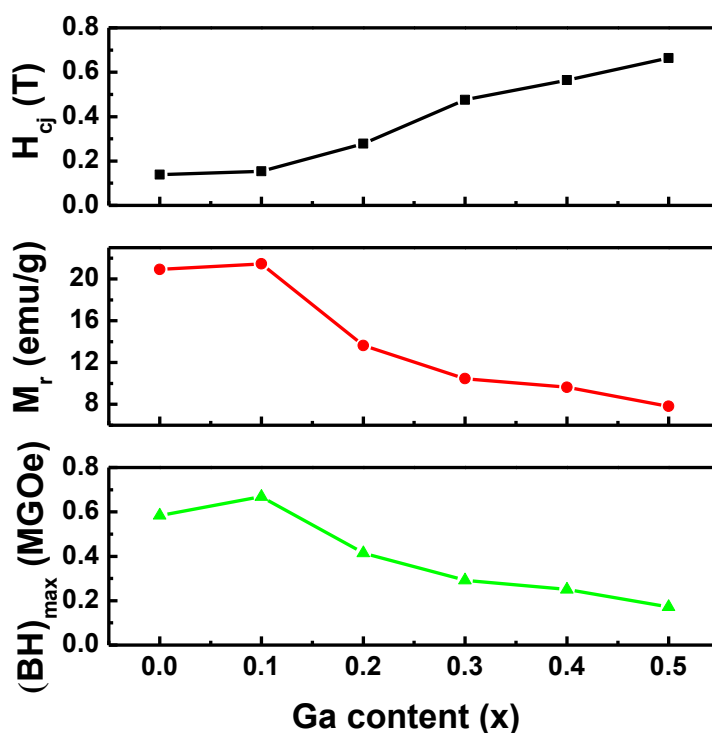
Figure 3. Magnetic properties (intrinsic coercivity H_{cj}, remanence M_r and maximum energy product $(BH)_{max}$) of MnBi$_{1-x}$Ga$_x$ alloys.
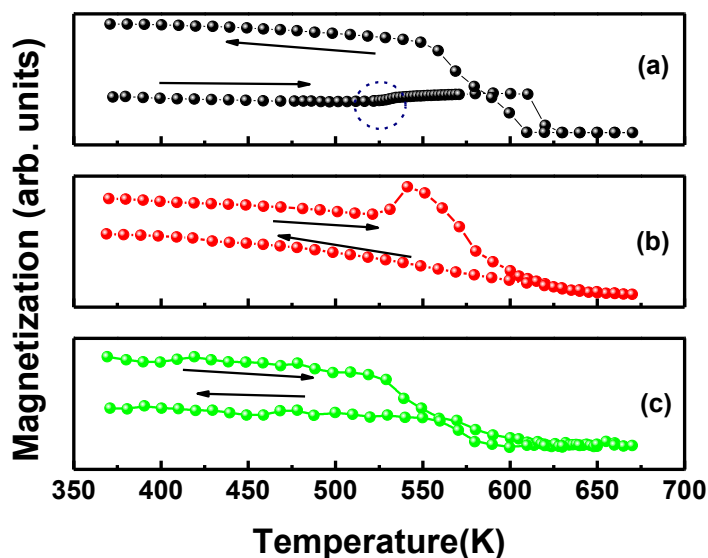

Figure 4. Magnetization as a function of temperature in the applied field of 500 Oe for MnBi$_{1-x}$Ga$_x$ alloys with (a) x = 0, (b) x = 0.1, and (c) x = 0.5.

Fig. 4 shows the magnetization as a function of temperature in the applied field of 500 Oe and the temperature is in the range of 370 K-670 K for MnBi$_{1-x}$Ga$_x$ alloys with (a) x = 0, (b) x = 0.1, and (c) x = 0.5, respectively. It shows that the magnetization of Ga-free MnBi decreases slowly during the

heating process and reaches the lowest value at 521 K (blue line of circle dashes) and then increases gradually up to 600 K. The increase of magnetization with temperature can be attributed to the formation of LTP-MnBi [17]. As the temperature exceeds 620 K, the magnetization of the alloy begins to decrease and drops dramatically to nearly zero. That is considered to be due to the magnetic phase transition of MnBi phase from LTP to paramagnetic high-temperature phase (HTP) [18-21]. As x = 0.1, the magnetization of the alloy decreases slowly and drops to nearly zero as the temperature at 607 K. During the cooling process, the magnetization of the alloy (x = 0.1) increases gradually. For the Ga-doped alloy with x = 0.5, it exhibits the similar phase transition. Meanwhile, during the cooling process for the Ga-doped alloy with x = 0.5, the magnetization maintains at a very low value at first. When the alloy is cooled to 590 K, its magnetization begins to increase, and phase transition HTP-LTP occurs in the alloy at this time. As the temperature drops to 550K, the magnetization of the alloy does not increase with the decrease of temperature, and its value remains relatively stable. In conclusion, the Curie temperature and the phase transition temperature of MnBi alloy decreases from low temperature to high temperature with the increase of Ga content.
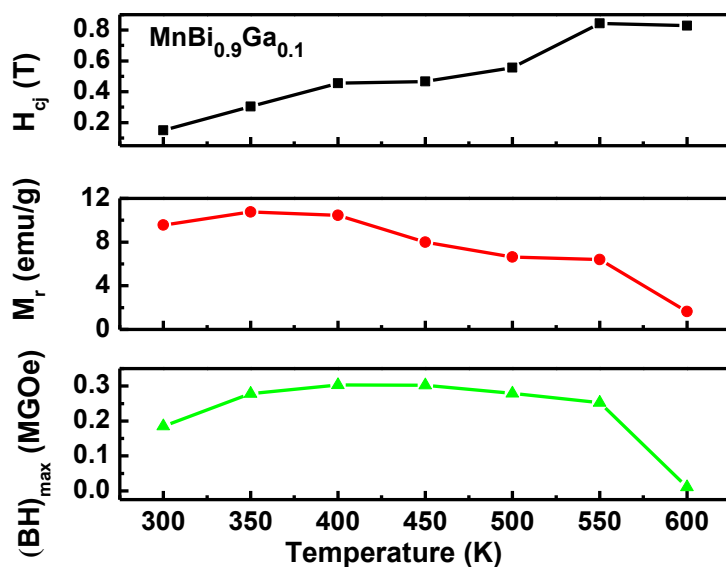

Figure 5. The temperature dependence of magnetic properties (H_{cj}, M_r and $(BH)_{max}$) for the MnBi$_{0.9}$Ga$_{0.1}$ alloy.

Furthermore, in order to study the effect of temperature on the magnetic properties of MnBi$_{1-x}$Ga$_x$ alloys, Fig. 5 show the temperature dependence of magnetic properties (H_{cj}, M_r and $(BH)_{max}$) for the MnBi$_{0.9}$Ga$_{0.1}$ alloy. It can be seen that the coercivity of the alloy at 300K is 0.149 T. During the heating process, the coercivity of the alloy increases gradually and reaches a maximum of 0.843 T at 550 K. As the temperature increases to 600 K, the coercivity of the MnBi$_{0.9}$Ga$_{0.1}$ alloy decreases slightly to 0.829 T. The coercivity temperature coefficient of the sample is β = 1.5 %/K in the temperature range of 100 K-600 K. It can be seen that the coercivity of the MnBi$_{0.9}$Ga$_{0.1}$ sample is closely related to temperature. The MnBi$_{0.9}$Ga$_{0.1}$ has a positive coercivity temperature coefficient in the range of 300 K to 600 K, which can be suitable applied in high temperature environment. The remanence M_r of the alloy varies slightly from 300 K to 400 K, and its value is 10.7 emu/g at 350 K.

As the temperature continues to rise, the remanence M_r of the alloy begins to decrease. As the temperature exceeds 550 K, the remanence M_r of the alloy decreases rapidly, and the value is 1.65 emu/g at 600K. The maximum energy product $(BH)_{max}$ of $MnBi_{0.9}Ga_{0.1}$ sample increased slightly at the beginning of heating temperature, reaching a maximum of 0.3 MGOe at 400 K. When the temperature continues to rise, the maximum energy product $(BH)_{max}$ of the alloy decreases slightly. As the temperature exceeds 550 K, the maximum energy product of the alloy decreases rapidly and decreases to 0.01 MGOe with the temperature of 600 K.
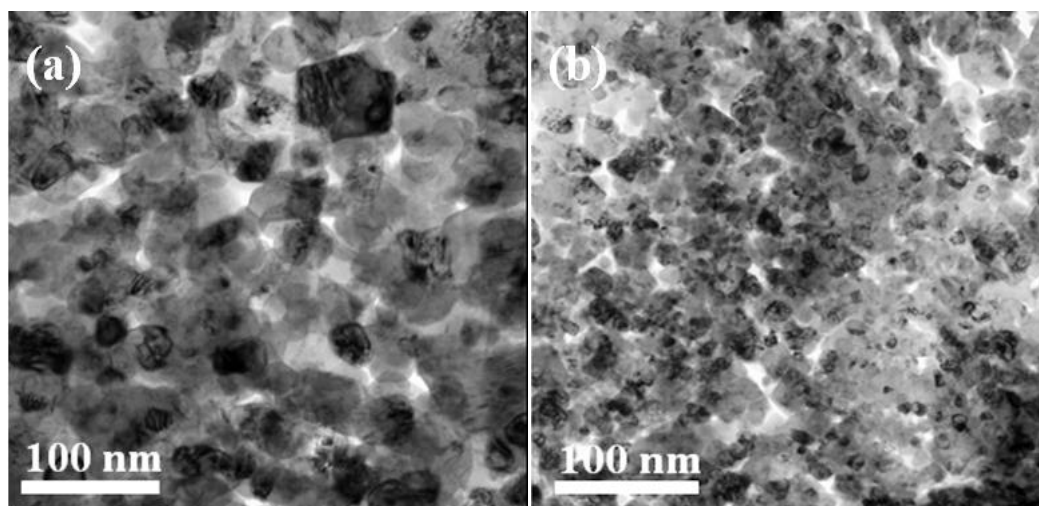

Figure 6. TEM images of the $MnBi_{1-x}Ga_x$ alloys with (a) x = 0 and (b) x = 0.1

In order to further understand the different magnetic properties of the Ga-free and Ga-doped samples, Fig. 6 shows the TEM images of the Ga-free (x = 0) and Ga-doped (x = 0.1) $MnBi_{1-x}Ga_x$ alloys. On comparing with Ga-free sample (Fig. 5 (a)), the Ga-doped (x = 0.1) sample (Fig. 5 (b)) obtains a more homogeneous microstructure. Additionally, by comparing the grain size for the Ga-free and Ga-doped alloys, it shows that the average grain size is 40±8 nm and 12±5 nm for the Ga-free and Ga-doped samples, respectively, which is consistent with the XRD results in the previous paper. It indicates that the Ga-doped sample has a smaller grain size and more homogeneous distribution of magnetic phases. The increase of H_{cj} and $(BH)_{max}$ for the Ga-doped sample in comparison with Ga-free sample may result from a smaller grain size and uniform distribution of magnetic phases.
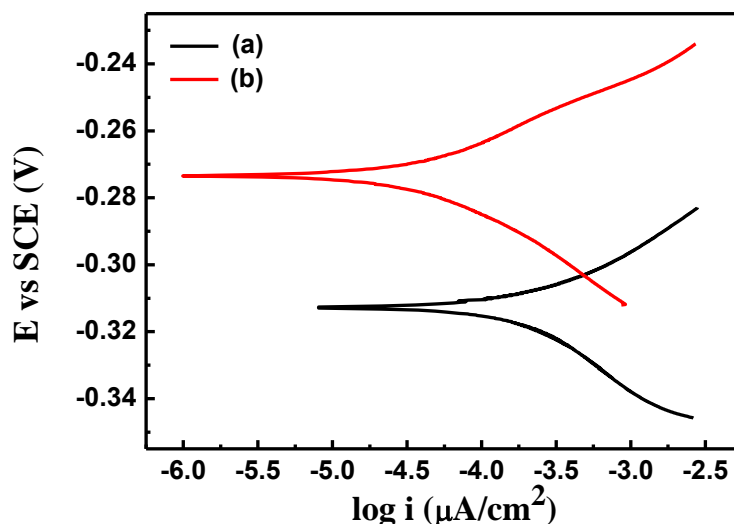
Figure 7. Polarization curves of the $MnBi_{1-x}Ga_x$ alloys with (a) x = 0 and (b) x = 0.1 tested in 2.5 wt.% NaCl aqueous solutions.

Table 1. The corrosion potential E_{corr} and corrosion current density i_{corr} of the $MnBi_{1-x}Ga_x$ alloys with x = 0 and x = 0.1.

Alloys	E_{corr}(V)	i_{corr}($\mu A/cm^2$)
x = 0	-0.301	101.32
x = 0.1	-0.252	29.35

Fig. 7 shows the potentiodynamic polarization curves of the $MnBi_{1-x}Ga_x$ alloys with (a) x = 0 and (b) x = 0.1 tested in 2.5 wt.% NaCl aqueous solutions. According to the potentiodynamic polarization curves, the corrosion potential E_{corr} and corrosion current density i_{corr} are calculated are showed in Table 1. The corrosion current density i_{corr} derived from Tafel curve for the Ga-free (x = 0) and Ga-doped (x = 0.1) $MnBi_{1-x}Ga_x$ alloys is 101.32 $\mu A/cm^2$ and 29.35 $\mu A/cm^2$, respectively. Meanwhile, the corrosion potential E_{corr} is increased from -0.301 V to -0.252 V as the Ga content is increased from x = 0 to x = 0.1. The higher value of corrosion potential E_{corr} and lower value of corrosion current density i_{corr} for the Ga-doped (x = 0.1) $MnBi_{1-x}Ga_x$ alloys, indicating that $MnBi_{1-x}Ga_x$ alloys with Ga-doped can remarkably improve the electrochemical stability and corrosion resistance in salt solution.

In conclusion, the present results demonstrated that the $MnBi_{1-x}Ga_x$ alloys with proper Ga-doped can improve the magnetic properties by due to the smaller grain size and uniform distribution of magnetic phases. Meanwhile, the corrosion resistance of the Ga-doped $MnBi_{1-x}Ga_x$ alloys can also be improved.

4. CONCLUSION

The effect of Ga content on the microstructure and magnetic properties of the $MnBi_{1-x}Ga_x$ (x = 0, 0.1, 0.2, 0.3, 0.4 and 0.5) alloys are studied. The present results demonstrated that the $MnBi_{1-x}Ga_x$ alloys with proper Ga-doped can improve the magnetic properties by due to the smaller grain size and uniform distribution of magnetic phases. Meanwhile, the corrosion resistance of the Ga-doped alloy can also be improved. The $MnBi_{1-x}Ga_x$ alloy that shows enhanced magnetic properties with $(BH)_{max} = 0.67$ MGOe is obtained as the Ga content at x = 0.1. With the increase of x, the coercivity increases gradually and reaches the maximum value (H_{cj}: 0.664 T) with x = 0.5, which is 4.8 times that of the Ga-free alloy (H_{cj}: 0.138 T). Furthermore, the MnBi alloy with Ga-doped obtains higher value of corrosion potential E_{corr} and lower value of corrosion current density i_{corr}, indicating that the corrosion resistance can also be improved with Ga-doped.

References

1. J.J. Croat, J.F. Herbst, R.W. Lee, F.E. Pinkerton, *Appl. Phys. Lett.,* 44 (1984) 148.
2. M. Sagawa, S. Fujimura, N. Togawa, H. Yamamoto, Y. Mutsuura, *J. Appl. Phys.,* 55 (1984) 2083.
3. Z.B. Li, B.G. Shen, M. Zhang, F.X. Hu, J.R. Sun, *J. Alloys Compd.,* 628 (2015) 325.
4. X. Li, Z. M. Ren, Y. Fautrelle, *Mater. Lett.,* 60 (2006) 3379.
5. Y. Yang, J.W. Kim, P.Z. Si, H.D. Qian, Y.H. Shin, X.Y. Wang, J.H. Park, O.L. Li, Q. Wu, H.L. Ge, C.J. Choi, *J. Alloys Compd.,* 769 (2018) 813.
6. S. Kim, H. Moon, H. Jung, S.-M. Kim, H.-S. Lee, C.-Y. Haein, W. Lee, *J. Alloys Compd.,* 708 (2017) 1245.
7. K. Kang, L.H. Lewis, A. R. Moodenbaugh, *J. Appl. Phys.,* 97 (2005) 10k302.
8. C. Guillaud, *J. Phys. Radium,* 12 (1951) 143.
9. T. Chen, W.E. Stutius, *IEEE Trans. Magn.,* 10 (1985) 581.
10. R.R. Heikes, *Phys. Rev.,* 99 (1955) 446.
11. J.B. Yang, K. Kamaraju, W.B. Yelon, W.J. James, Q. Cai, A. Bollero, *Appl. Phys. Lett.,* 79 (2001) 1846.
12. D.T. Zhang, S. Cao, M. Yue, W.Q. Liu, J.X. Zhang, Y. Qiang, *J. Appl. Phys.,* 109 (2011) 07A722.
13. G. K. Williamson, *Acta. Metall.,* 1 (1953) 23.
14. P.E. Kelly, K. O'Grady, P.I. Mayo, R.W. Chantrell, *IEEE Trans. Magn.,* 25 (1989) 3881.
15. J. Lyubina, K.H. Müller, M. Wolf, U. Hannemann, *J. Magn. Magn. Mater.,* 322 (2010) 2948.
16. S.Y. Zhang, P.Y. Zhang, H.C Jiang, Y.J. Shi, N.J. Yu, H.L. Ge, *J. Magn.,* 19 (2014) 205.
17. S. Saha, R. T. Obermyer, B. J. Zande, V. K. Chandhok, S. Simizu, S. G. Sankar, J. A. Horton, *J. Appl. Phys.,* 91 (2002) 8525.
18. Y.B. Yang, X.G. Chen, S. Guo, A.R. Yan, Q.Z. Huang, M.M. Wu, D.F. Chen, Y.C. Yang, J.B. Yang, *J. Magn. Magn. Mater.,* 330 (2013) 106.
19. R.F. Sabiryanov, S.S. Jaswal, *J. Appl. Phys.,* 85 (1999) 5109.
20. J.T. Li, M.X. Pan, Y.D. Yu, H.L. Ge, Q. Wu, Int. J. Electrochem. Sc., 13 (2018) 8897.
21. V.V. Ramakrishna, S. Kavita, Ravi Gautam, T. Ramesh, R. Gopalan, *J. Magn. Magn. Mater.,* 458 (2018) 23.